JACS
JOURNAL OF THE AMERICAN CHEMICAL SOCIETY
Article
pubs.acs.org/JACS

Release of High-Energy Water as an Essential Driving Force for the High-Affinity Binding of Cucurbit[*n*]urils

Frank Biedermann,[†] Vanya D. Uzunova,[‡] Oren A. Scherman,[†] Werner M. Nau,[‡] and Alfonso De Simone*[,§]

[†]Melville Laboratory for Polymer Synthesis and Department of Chemistry, University of Cambridge, Lensfield Road, Cambridge, CB2 1EW, U.K.

[‡]School of Engineering and Science, Jacobs University Bremen, Campus Ring 1, 28759 Bremen, Germany

[§]Division of Molecular Biosciences, Imperial College London, South Kensington, SW7 2AZ, U.K.

Supporting Information

ABSTRACT: Molecular dynamics simulations and isothermal titration calorimetry (ITC) experiments with neutral guests illustrate that the release of high-energy water from the cavity of cucurbit[*n*]uril (CB*n*) macrocycles is a major determinant for guest binding in aqueous solutions. The energy of the individual encapsulated water molecules decreases with increasing cavity size, because larger cavities allow for the formation of more stable H-bonded networks. Conversely, the total energy of internal water increases with the cavity size because the absolute number of water molecules increases. For CB7, which has emerged as an ultrahigh affinity binder, these counteracting effects result in a maximum energy gain through a complete removal of water molecules from the cavity. A new design criterion for aqueous synthetic receptors has therefore emerged, which is the optimization of the size of cavities and binding pockets with respect to the energy and number of residing water molecules.

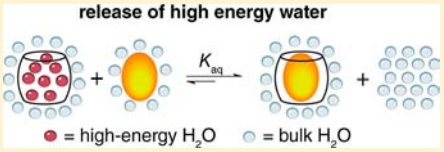

INTRODUCTION

Artificial receptor molecules such as water-soluble macrocyclic hosts have received considerable interest due to promising applications in molecular recognition and sensing, materials chemistry, and drug delivery systems and as mimicks of enzymatic catalysis.[1] Several supramolecular strategies for designing synthetic systems with improved host–guest binding have been exploited, including the optimization of direct host–guest interactions via hydrogen bonds (H-bonds), electrostatic and van der Waals (vdW) interactions,[2−8] and the maximization of the hydrophobic effect[4,7,9−11] and the exploitation of cohesive solvents.[12,13] The binding of these designed systems falls short, however, when compared to the high-affinity binding of cucurbit[*n*]urils (CB*n* with n = 5−8,10),[14,15] a class of structurally simple macrocycles with exceptional binding properties (Chart 1). In particular, CB7 stands out among all macrocycles due to its ultrahigh affinity binding,[16−19] which is rivaled only by the biological biotin–avidin pair.[20] Suprisingly, neutral charged guests show high affinity, K_a up to 10^{10} M^{-1} with CB*n*,[18,19] whereas for other synthetic supramolecular systems similar affinities in water can only be reached for the interaction between highly charged hosts and (oppositely) highly charged guests, for example, in the binding of nucleotide triphosphates by peraminocyclodextrins.[21−23]

To rationalize CBn complexation, numerous literature reports have already demonstrated the importance of size complementary, the hydrophobic effect (entropic gain from water release upon binding), and direct host–guest interactions such as the well-documented ion–dipole interactions of positively charged residues with the carbonyl rim of CB homologues, in particular ammonium groups.[6,15,24] Nevertheless, the question why these rigid barrel-shaped macrocycles display such an exceptionally strong binding even with uncharged guests, and, in particular, why the intermediary sized CB7 shows maximum binding when compared to its smaller homologue CB6 and its larger one CB8, is not understood.[25,26] Consequently, by extending hypotheses originally advanced for for cyclophanes and cyclodextrins,[4,7,27] we concluded that additional factors, in particular the confinement of water molecules in the host cavity *prior* to guest binding, should be considered. Confined water molecules assume peculiar properties that can significantly diverge from the bulk.[28−32] For example, experiments and simulations of confined water molecules in reversed micelles have revealed their altered dynamic properties, in particular when their accessible space was reduced.[33−36] Moreover, the properties of

Chart 1. Cucurbit[*n*]uril (CB*n*) macrocycles

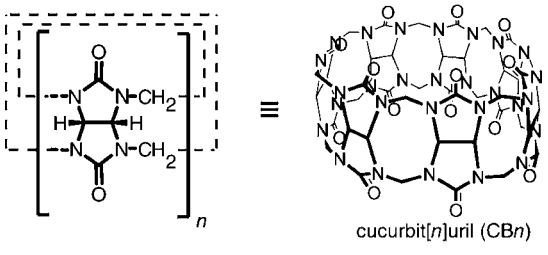

Received: April 11, 2012
Published: August 11, 2012

dx.doi.org/10.1021/ja303309e | J. Am. Chem. Soc. 2012, 134, 15318−15323

Table 1. Calculated Properties of CB*n* Cavity Water Molecules As Compared to the Bulk

	bulk water	CB5[a]	CB6	CB7	CB8
cav. vol[b] (Å^3)		45 [68][c]	118 [142][c]	214 [242][c]	356 [367][c]
$N(H_2O)$[d]		2.0 (1.0) [2][c]	3.3 [4][c]	7.9 [8][c]	13.1 [12][c]
PC (%)[e]	55	76 (38)	47	64	63
t_{res} (ps)[f]	21	>1000[f]	363	529	449
H-bond-count[g]	2.54	0.99 (0.00)	1.31	2.01	2.55
$E_{pot}(H_2O)$ (kJ/mol)[h,i]	79.0 ± 15.2	63.2 ± 14.0 (49.9 ± 5.8)	64.4 ± 11.0	74.4 ± 11.3	81.1 ± 12.5
$E_{DFT}(H_2O)$ (kJ/mol)[h,j]		79.3 (61.8)	90.2	96.6	137.1
ΔE_{pot}(all) (kJ/mol)[k]	reference	−41.6 ± 28.8 (−29.1 ± 15.2)	−51.1 ± 29.0	−102.4 ± 31.3	−66.2 ± 10.7

[a]CB5 cavity water molecules do not exchange with the bulk during 20 ns of MD simulation time. See Supporting Information for details. [b]CB*n* cavity volume calculated via Monte Carlo particle insertion with CB*n* cavity borders defined as $z = \pm 3.2$ Å, see Supporting Information for details. [c]Cavity values from ref 26 are given in square brackets. [d]Average number of cavity water molecules. [e]Packing coefficient = [$N(H_2O)$(water vdW volume)]/(cav vol). [f]Residence times of water molecules determined by a single-exponential fit to an autocorrelation function. [g]Average number of hydrogen bonds between adjacent water molecules; H bonds were considered if O···O distance ≤3.5 Å and O−H−O angle ≤150° between neighboring water molecules. [h]Average potential energy loss when a single water molecule is removed. [i]From MD simulations. [j]From B3LYP/6-31G* SP calculations, see Supporting Information for details. [k]Difference in potential energy for the removal of all cavity water and transfer of those to a spherical cavity in the aqueous bulk; see also Supporting Information Figure S5.

confined water molecules are key modulators of host−guest affinities[37,38] and are often utilized in biological processes[39−41] such as assisting protein folding[42] or protein−protein and protein−ligand interactions.[43−48] Herein, we demonstrate through simulations and experiments that the major driving force for complexation of hydrophobic residues with CB*n* stems from a solvent effect, namely, the release of "high-energy" water, that is, enthalpically and entropically unfavorable water molecules in the CB cavities.

RESULTS

Hydration Properties of CB*n*. The hydration patterns of CB*n* molecules (with *n* ranging from 5 to 8) have been investigated in detail by molecular dynamics (MD) simulations to assess the nature of changes in the structure, dynamics, and thermodynamics of the internal water molecules upon guest binding. The calculations were performed with the GROMACS package.[49] Three different water models (tip3p, tip4pEW, and tip5p) were used in independent simulations to provide a robust analysis of the properties of CB*n* hydration. In order to correctly account for dispersion interactions in CB−guest inclusion complexes, in particular, and Lennard-Jones interactions, in general, the amber99SB parameters were recalibrated by using MP2/6-31G* calculations (see Supporting Information for details). In essence, the atomic polarizabilities of the force field need to be reduced in order to match the low polarizability of the CB cavity, which has been experimentally established.[26] For example, the radiative lifetimes of chromophores, which follow Einstein's law for spontaneous emission and depend on the refractive index (the polarizability of the environment) are much longer inside CB7 than those in any condensed phase.[26,50]

The simulations of CB*n* molecules were analyzed to elaborate on the structure and dynamics of internal water molecules (see Table 1 for tip5p water model, and Supporting Information, Tables S2 and S3 for tip3p and tip4pEW). Residence times (t_{res}) of the water molecules in the CB*n* cavities were found to be at least 1 order of magnitude longer than in the bulk. In agreement with the known behavior of water molecules in the proximity of hydrophobic surfaces[51] or in the interior of reverse micelles,[34] the cavity water showed also a longer relaxation time for the reorientation of its dipole (Supporting Information, Figure S4).

Moreover, in the case of CB5, CB6, and CB7, water−water interactions in the CB*n* cavity were substantially less favorable than in the bulk, which can be traced back to (*i*) an impaired ability to optimize hydrogen bond networks within the very small cavities (H-bond-count in Table 1) and (*ii*) a less favorable potential energy, $E_{pot}(H_2O)$ in Table 1. The latter effect is mainly due to weaker Coulombic (mainly dipole−dipole) water−water interactions of water molecules inside the CB*n* cavities, which are insufficiently counterbalanced by the relatively weaker electrostatic interactions of the included water molecules with the nonpolar CB*n* cavity (see Supporting Information Table S4). For example, in the case of CB6, only a few H-bonds between internal water molecules can be established through a linear/rectangular arrangement involving 3 to 4 molecules in the cavity, leading to a preferential alignment (Figure 1) as a consequence of spatial confinement.

In contrast to the smaller homologues, the calculations suggest that water molecules in the interior of CB8 are able to optimize their H-bond network to a degree that is structurally similar to that of the bulk phase (Table 1). Indeed, the energy for removal of the first water molecule from the inside of CB8 is comparable to that required for removing a water molecule

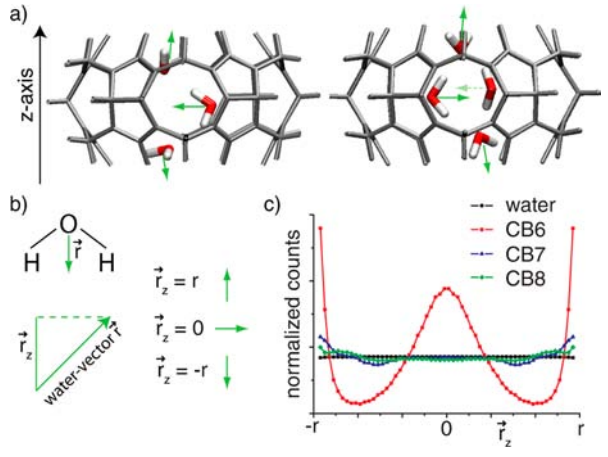

Figure 1. (a) Representative arrangements of three (left) or four (right) water molecules in the CB6 cavity. (b) Definition of the water vector. (c) Calculated distributions of the water vectors inside the CB cavities and in bulk water (tip5p water model).

dx.doi.org/10.1021/ja303309e | J. Am. Chem. Soc. 2012, 134, 15318−15323

from the bulk solution (Table 1, $E_{pot}(H_2O)$). However, the total energy for removing all internal water molecules, ΔE_{pot}(all) in Table 1, is still smaller than the energy for removing a water cluster of the same size from the bulk. Density functional theory (DFT) calculations, performed on representative configurations from the MD simulations, also yielded the most stable internal water network in CB8 (see Table 1 and Scheme 1). The water inside the CB8 cavity shows also longer relaxation times of water dipole orientations. This points to an enhanced water pairing effect,[51] which is maximal for CB8 (Supporting Information Figure S4).

Another peculiarity of CB8 hydration is a cavitation in the internal water structure leading to an empty volume of approximately 3.5 Å in diameter. This is surprising, because this volume would be sufficiently large to accommodate another water molecule (see Supporting Information Figure S2). Voids in water are extremely unusual, which is often summarized as "nature abhors a vacuum". Control simulations in which one or two water molecules were inserted into this empty volume led to a rapid reappearance of the void after a few picoseconds of MD simulation. Note that the cavitation effect is invariant to MD parameter sets, including higher values for the Lenard-Jones-parameters, turning-off the partial charges of the CB8 atoms, and the solvent models (tip5p, tip4pEW, and tip3p). Thus, it can be assumed that the formation of the void in the hydration pattern of CB8 is caused by specific geometric effects. Furthermore, the CB8 cavity displayed the slowest relaxation rates of cavity water−dipole orientation while a control simulation, in which a water was restrained to occupy the void in the center of the CB8 cavity, resulted in a much faster relaxation (Figure S2), suggesting that the inner water molecules in the unperturbed CB8 cavity are associated with a pronounced water pairing effect[51] (see further discussions in the Supporting Information).

Role of Solvent in Host−Guest Binding by CB*n*. The observed high energy of the water molecules within the CB cavities provides an essential driving force for host−guest complexation (Scheme 1). As an important insight, the

Scheme 1. Release of High Energy Water Molecules upon Binding

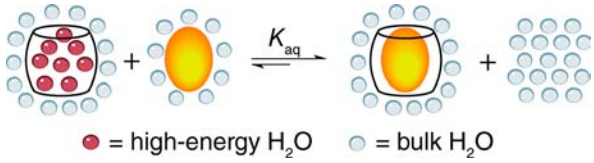

calculated potential energy of release of all internal water molecules (ΔE_{pot}(all)) reaches a maximum for CB7 since the size (diameter) of the CB7 cavity does not allow for the cavity water molecules to arrange in an energetically stable H-bonded cluster (as found for CB8) while requiring a larger number of water molecules than for CB6 to fill the cavity. Therefore, a delicate interplay between energetic frustration and the absolute number of cavity water molecules in CB7, as depicted schematically in Scheme 1, may provide an explanation of why the medium-sized macrocycle CB7 shows the highest binding constants known for synthetic macrocycles in general.

To test our model in further detail, the thermodynamics of complex formation was investigated for selected guests by isothermal titration calorimetry (ITC). The criteria of guest selection included the absence of charged groups in order to neglect ion-dipole interactions with the carbonyl rims of the CB*n* and a polar nature of the guest to ensure sufficient solubility for ITC experiments. Additionally, only weakly basic guests were considered in order to reduce H-bonding of the guest with the solvent. While the experimentally determined enthalpy (ΔH) does not directly correspond to the force-field potential energy of the system, we assume both physical quantities to be correlated. Accordingly, the computed release of internal water molecules would correspond to exothermic binding, as their potential energy is higher than that of the bulk. Indeed, for all CB6 complexes investigated (in which according to MD calculations all water molecules are displaced from the cavity) our measurements yielded an exothermic binding (Table 2). In contrast, the calculated potential energies of the guests (ΔE_{pot}(guest)), defined as a difference in the direct interaction energy of the guest with water and with the host, that is, prior and after complex formation, showed no unifying trends (see Table 2 and Supporting Information Figure S6). For example dimethylsulfoxide (DMSO), *N*,*N*-dimethylformamide (DMF), and pyrrole have more favorable potential energies in bulk water than in the CB6 cavity. This suggests that a solvent effect, and not direct interactions between host and guest, dominates the trends in ΔH as well as in the absolute host−guest affinities. Consistent with the results for CB6, ITC measurements with CB7 showed that the binding of all guests is also strongly exothermic, whereas the calculated ΔE_{pot}(guest) values are only in one instance (CB7-pyrrole) indicative of a stabilization upon binding. This supports the idea that in the majority of cases the favorable enthalpic contribution arises from the release of internal water molecules. The entropic contribution for CB7 complex formation is smaller in magnitude and mostly of different sign than for CB6 with the same guest. These measurements are in agreement with the MD simulations showing that the cavity water molecules in CB6 have highly restricted orientations (Figure 1), which suggests a significant entropic gain (orientational and translational terms) due to their release upon complex formation.

The aforementioned very small guests produced, on the other hand, insufficient heat effects with CB8, which precluded ITC experiments in these cases (see Supporting Information Figure S7 for representative examples). Whether this is due to a negligible binding or to very small enthalpies of binding (the latter would be expected from the distinctly lower energy of the water molecules inside CB8) could not be readily judged in these cases. To directly compare CB7 and CB8 in the complexation of the same guest, 2,3-diazabicycloc[2.2.2]oct-2-ene (DBO) was used as it forms 1:1 complexes with both CB7 and CB8 (but not with CB6).[50,52] Overall binding enthalpies of −75 ± 1 kJ/mol for CB7 and −37 ± 1 kJ/mol for CB8 were determined by ITC; solvent isotope effects were found to be small.[53]

A structural explanation of these measurements arises from our MD simulations, which show that the binding of DBO leads to the release of all inner water molecules from CB7 while nine internal water molecules remain inside the CB8 cavity and percolate the DBO guest (Figure 2A). The presence of residual cavity water molecules in CB8·DBO is also one possible explanation for the smaller fluorescence lifetime of the DBO fluorophore in its CB8 than in its CB7 complex (τ = 415 ns in H_2O, 830 ns in its CB7 complex, and 770 ns in its CB8 complex; see Supporting Information for details). Overall, the energetic contribution of the release of high-energy water

dx.doi.org/10.1021/ja303309e | J. Am. Chem. Soc. 2012, 134, 15318−15323

Table 2. Thermodynamic Data and MD Calculated Properties of CB*n* Complexes with Neutral Guests

	K_a (10^3 M^{-1})	ΔH^a (kJ/mol)	$-T\Delta S^a$ (kJ/mol)	ΔE_{pot}(guest)^b (kJ/mol)	$N(H_2O)^c$	PC^d (%)	$E_{pot}(H_2O)^e$ (kJ/mol)
CB6·DMSO	1.2 ± 0.3	−5 ± 1	−24 ± 3	7.1	0.0	71	
CB7·DMSO	0.13 ± 0.02	−14 ± 1	2 ± 2	6.3	2.4	60	68.5
CB6·DMF	1.8 ± 0.3	−6 ± 1	−24 ± 3	0.4	0.0	64	
CB7·DMF	0.61 ± 0.02	−22 ± 1	6 ± 2	7.4	1.9	53	78.7
CB6·acetone	7.2 ± 0.3	−11 ± 2	−11 ± 4	−7.5	0.0	55	
CB7·acetone	0.64 ± 0.02	−13 ± 1	−1 ± 2	−3.5	2.1	49	62.1
CB6·pyrrole	36 ± 3	−23 ± 2	−3 ± 4	10.2	0.0	60	
CB7·pyrrole	1.7 ± 0.2	−30 ± 1	11 ± 2	−31.6	3.2	61	72.9
CB7·DBO^f	13400 ± 200^g	−75 ± 1	34 ± 2	−9.6	0.0	55	-
CB8·DBO^f	16 ± 3	−37 ± 1	13 ± 3	−17.0	9.2	75	78.4
CB7·cyclopentanone	330 ± 0.2	−41 ± 1	9 ± 2	−6.4	0.3	45	67.0
CB8·cyclopentanone	1.1 ± 0.2	−35 ± 1	18 ± 2	14.1	6.2	54	74.5

[a]Measured by ITC in aqueous solution at 25 °C, fitted according to a 1:1 binding stoichiometry. [b]Change in direct interaction energy of the guest with its environment (CB*n* and water) upon complex formation, $\Delta E_{pot}(guest) = [E_{pot}(CBn{:}guest) + E_{pot}(water{:}guest)]_{bound} - [E_{pot}(CBn{:}guest) + E_{pot}(water{:}guest)]_{free}$, see also Figure S6 in Supporting Information. [c]Number of residual cavity water molecules in the host−guest complex. [d]Packing coefficient, $PC = [N(H_2O)\cdot(\text{water vdW volume}) + (\text{guest vdW volume})]/(\text{cav. vol})$. [e]Average energy required to remove one water molecule from cavity of the host−guest complex. [f]DBO: 3-diazabicycloc[2.2.2]oct-2-ene. [g]This value is slightly higher than that reported in ref 52, presumably because of the use of a different CB7 sample.

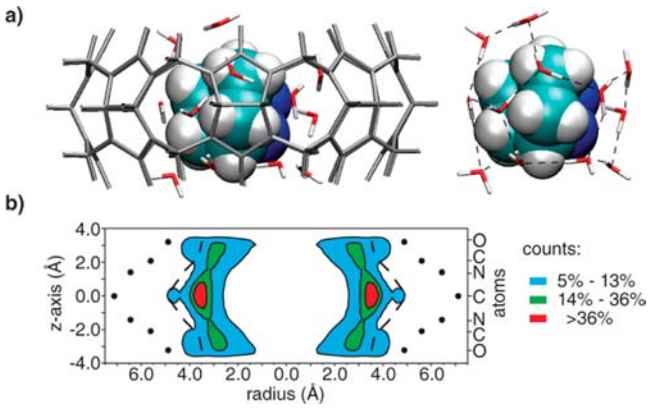

Figure 2. (a) Representative snapshot of the CB8·DBO complex and residual cavity water molecules (left). H-bonds are indicated by dashed lines, the CB8 atoms have been removed for clarity (right). (b) Distribution of the residual cavity water molecules in the CB8·DBO complex. Black dots show the location of CB8 atoms, the dashed line shows the corresponding inner vdW surface.

molecules is lower for CB8 than for CB7 since both the number and the energetic gain per released water molecule is smaller. Similar conclusions can be drawn when comparing the thermodynamic values of CB7 and CB8 complex formation with cyclopentanone (Table 2). Furthermore, for the smallest guests immersed in the larger cavities (CB7 and CB8), additional water molecules would be needed to achieve an ideal packing (i.e., 55% according to Rebek's empirical rule[54]). Nevertheless, the $E_{pot}(H_2O)$ values for the hydrated CB*n*·guest·$(H_2O)_n$ complexes (Table 2) are less favorable than those of CB*n* and the bulk in most cases (Table 1). Consequently, these "residual" cavity water molecules in CB8 exhibit a negative influence on the energetic balance for the formation of these CB*n*−guest complexes. Thus, complementary sizes between host and guest are not only of importance to strengthen the direct binding forces but are equally necessary to avoid frustrated interstitial water molecules in the host−guest complex.

It is worth mentioning that a high enthalpic gain of similar magnitude (approximately −90 kJ/mol) to that of CB7·DBO is also the major energetic contributor to the ultrahigh binding affinity of ferrocene derivatives with CB7 as was reported by Rekharsky et al.[19] Both ferrocene and DBO possess the correct size and shape to replace all water molecules from the CB7 cavity while filling the cavity space to approximately 55%, in agreement with Rebek's rule.[54]

DISCUSSION

Knowledge of the precise structure and energy of the water molecules residing in the inner cavity of CB*n* is indispensable for a comprehensive understanding of their host−guest complexation behavior.[24−26] The present investigation demonstrates that the release of high-energy and, particularly in the case of CB6, highly ordered water molecules constitutes a major driving force for the inclusion of neutral residues into CB*n*. This revives earlier hypotheses, derived from analyses of crystal structure data for cyclodextrins, on the importance of high-energy water in host−guest complexation processes.[4,7] Indeed, while the high binding affinities of CB*n* have frequently been correlated with direct host−guest interactions,[17,55,56] the examples described herein show that these interactions alone *cannot* account for the large exothermic binding. Conversely, when considering the energetic contribution of the release of cavity water, both the exothermic nature of binding and the differences between CB6 and CB7 can be rationalized (Table 2). For the guests herein studied, the average number of high-energy water molecules that are released upon binding is larger (i.e., roughly double, Supporting Information, Tables S5 and S6) for CB7 than for CB6, which is in agreement with the larger absolute values of ΔH measured for complexation by CB7. Thus, although the enthalpy of the individual high-energy water molecules in the smaller CB6 cavity is higher than those inside CB7, the total energy for removal of all high-energy water molecules from CB7 is higher on account of a more than twice as large the number of water molecules released upon binding, see ΔE_{pot}(all) values in Table 1. As a result, the intermediate size of CB7 appears to provide the perfect compromise between the number and energy of encapsulated water molecules in order to allow for the maximum energetic gain upon guest binding and the concomitant water release from the macrocycle. The convergence of the results from

dx.doi.org/10.1021/ja303309e | J. Am. Chem. Soc. 2012, 134, 15318−15323

simulations employing different water models and different parametrization schemes for the CB*n* hosts (including the removal of Coulombic and vdW interactions) suggests that the unusual properties of water molecules in the CB*n* cavities are mainly due to specific geometrical effects that result in an enthalpically as well as entropically unfavorable water confinement.

CONCLUSIONS

The largest energy gain in the course of the complexation between neutral guests and CB*n* hosts occurs when (*i*) all water molecules are removed from the cavity and (*ii*) the water molecules to be displaced from the host cavity upon binding possess high energy. This combination emerges as a key criterion for the design of high-affinity synthetic receptors. The ultrahigh affinity binders for CB7, such as adamantyl[16] and ferrocenyl[17] ammonium derivatives, fulfill this combination through the immersion of the hydrophobic cores and further benefit from additional direct host–guest interactions such as ion–dipole forces. Our finding opens the challenge to design concave hosts with even higher binding affinities in water by maximizing the total energy of the included water cluster.

MATERIALS AND METHODS

Simulations Setup. MD simulations were carried out with the Gromacs package[49] by using a modified parametrization of the all-atom amber99sb forcefield[57,58] and tip3p and tip4pEW as well as tip5p explicit water models.[59] The simulations were carried out in NPT ensemble with periodic boundary conditions at a constant temperature of 300 K. A rectangular box (3.5 nm edge-length) was used for accommodating the CB*n*, guest molecule (when employed), and water molecules (see Supporting Information Table S1). A time step of 1.0 ps was employed. All simulations were carried out for a time of 20 ns after the system was equilibrated for 10 ns. As the hydration of small molecules equilibrates on the time scale of picoseconds, the simulated time was sufficiently long to provide a robust statistics for the CB*n* solvation. The V-rescale algorithm was applied for the temperature and Berendsen pressure coupling. The bonds were constrained by the Lincs algorithm. The particle-mesh Ewald (PME) method was used to account for the electrostatic contribution to nonbonded interactions (grid spacing of 0.12 nm).

Hydration Analysis: Solvent Density Map. The MD samplings were analyzed to compute solvent density maps whose maxima represent the molecular dynamics hydration sites (MDHS).[43,60] For each frame of the sampling, the positions of the water molecules were counted in a grid of 0.5 Å after superimposing the current host–guest structure onto a reference one. The maps were stored in EDM format and drawn by means of curve levels.

DFT Calculations of the Hydrated CB*n*. DFT calculations were performed using the Spartan08 software package from Wavefunction. Representative configurations of water molecules within the CB*n* cavities as obtained from snapshots of the MD simulations were used as starting structures. Prior to single point (SP) calculation (B3LYP/6-31G*) of the energies, the positions of the hydrogen atoms of the water molecules were geometry optimized (by keeping the position of all other atoms fixed) to relieve some strain from the water molecules and to allow them to "optimize" their H-bond network. Subsequently, one water atom was removed from the cavity and the SP energy was calculated. The difference in SP energies prior and after removal of the cavity water molecule corresponds to the energetic stabilization of this water molecule in the CB*n* cavity. This process was permuted through all of the water molecules in the CB*n* cavity, and the averaged energies are reported in Table 1. The same steps were also performed on the water clusters alone (i.e., after removing all CB*n* atoms) to double-check that the trends in the stabilization of the water molecules within CB5–CB8 were on account of differences in the water–water interactions and did not result from apparent differences of water–CB*n* interactions (such as VdW interactions). Indeed, the same trends were found in the presence and absence of CB*n* with the same arrangement of the (cavity) water atoms.

Materials and Isothermal Titration Calorimetry. All starting materials were purchased from Alfa Aesar and Sigma Aldrich and used as received unless stated otherwise. CB6, CB7, and CB8 were synthesized according to literature methods.[14] DBO was prepared as reported.[61] Isothermal titration experiments were carried out on a VIP-ITC instrument from Microcal, Inc. at 25 °C in water. The binding equilibria were studied using a cellular CB*n* concentration of 0.04 mM for CB6 and CB8, 0.2 mM for CB7, to which a ten times more concentrated guest solution was titrated. Typically 20–30 consecutive injections of 10 μL of each were used. All solutions were degassed prior to titration. Heats of dilution were determined by titration of the guest solution into water. The first data point was always removed from the data set prior to curve fitting. The data were analyzed by using the Origin 7.0 software with the one-set-of-sites model. The knowledge of the complex stability constant (K_a) and molar reaction enthalpy (ΔH°) enabled the calculation of the standard free energy (ΔG°) and entropy changes (ΔS°) according to $\Delta G^\circ = -RT \ln K_a = \Delta H^\circ - T\Delta S^\circ$.

Fluorescence Lifetime Measurements. The fluorescence lifetimes of free and complexed DBO were measured on a time-correlated single photon counting (TCSPC) fluorometer (F 900, Edinburgh Instruments). Typically, 10^4 counts were collected at the peak channel, and the decay curves were fitted by least-squares reconvolution with the instrumental software; the quality of the parameters was judged by the reduced χ^2 values (<1.1) and the randomness of the weighted residuals.

ASSOCIATED CONTENT

Supporting Information

Detailed procedures for the force field parametrization of the CB*n* and guest molecules, for the analysis of the computed hydration maps, and for the DFT simulations are given; coordinates and energies of DFT minimized molecules; supporting Figures S1–S10; supporting Tables S1–S8. This material is available free of charge via the Internet at http://pubs.acs.org.

AUTHOR INFORMATION

Corresponding Author

a.de-simon@imperial.ac.uk

Notes

The authors declare no competing financial interest.

ACKNOWLEDGMENTS

We acknowledge Prof. Daan Frenkel (University of Cambridge) and Dr. Sean Ohlinger (Wavefunction, Inc.) for helpful discussions and comments. This work was supported by the German Academic Exchange Service (DAAD) (F.B.), EPSRC (A.D. and O.A.S.), DFG (V.D.U. and W.M.N.), and the Leverhulme foundation (O.A.S. and W.M.N.).

REFERENCES

(1) Oshovsky, Gennady V.; Reinhoudt, David N.; Verboom, W. *Angew. Chem., Int. Ed.* **2007**, *46*, 2366–2393.
(2) Haj-Zaroubi, M.; Mitzel, N. W.; Schmidtchen, F. P. *Angew. Chem., Int. Ed.* **2002**, *41*, 104–107.
(3) Hunter, C. A. *Angew. Chem., Int. Ed.* **2004**, *43*, 5310–5324.
(4) Schneider, H.-J. *Angew. Chem., Int. Ed.* **2009**, *48*, 3924–3977.
(5) Schneider, H.-J.; Yatsimirsky, A. K. *Chem. Soc. Rev.* **2008**, *37*, 263–277.
(6) Houk, K. N.; Leach, A. G.; Kim, S. P.; Zhang, X. *Angew. Chem., Int. Ed.* **2003**, *42*, 4872–4897.
(7) Schneider, H.-J. *Angew. Chem., Int. Ed.* **1991**, *30*, 1417–1436.

(8) Hunter, C. A.; Sanders, J. K. M. *J. Am. Chem. Soc.* **1990**, *112*, 5525−5534.
(9) Inoue, Y.; Liu, Y.; Tong, L. H.; Shen, B. J.; Jin, D. S. *J. Am. Chem. Soc.* **1993**, *115*, 10637−10644.
(10) Southall, N. T.; Dill, K. A.; Haymet, A. D. J. *Chem. Phys. B* **2002**, *106*, 521−533.
(11) Widom, B.; Bhimalapuram, P.; Koga, K. *Phys. Chem. Chem. Phys.* **2003**, *5*, 3085−3093.
(12) Smithrud, D. B.; Wyman, T. B.; Diederich, F. *J. Am. Chem. Soc.* **1991**, *113*, 5420−5426.
(13) Smithrud, D. B.; Diederich, F. *J. Am. Chem. Soc.* **1990**, *112*, 339−343.
(14) Kim, J.; Jung, I. S.; Kim, S. Y.; Lee, E.; Kang, J. K.; Sakamoto, S.; Yamaguchi, K.; Kim, K. *J. Am. Chem. Soc.* **2000**, *122*, 540−541.
(15) Lagona, J.; Mukhopadhyay, P.; Chakrabarti, S.; Isaacs, L. *Angew. Chem., Int. Ed.* **2005**, *44*, 4844−4870.
(16) Mukhopadhyay, P.; Zavalij, P. Y.; Isaacs, L. *J. Am. Chem. Soc.* **2006**, *128*, 14093−14102.
(17) Jeon, W. S.; Moon, K.; Park, S. H.; Chun, H.; Ko, Y. H.; Lee, J. Y.; Lee, E. S.; Samal, S.; Selvapalam, N.; Rekharsky, M. V.; Sindelar, V.; Sobransingh, D.; Inoue, Y.; Kaifer, A. E.; Kim, K. *J. Am. Chem. Soc.* **2005**, *127*, 12984−12989.
(18) Florea, M.; Nau, W. M. *Angew. Chem., Int. Ed.* **2011**, *50*, 9338−9342.
(19) Rekharsky, M. V.; Mori, T.; Yang, C.; Ko, Y. H.; Selvapalam, N.; Kim, H.; Sobransingh, D.; Kaifer, A. E.; Liu, S.; Isaacs, L.; Chen, W.; Moghaddam, S.; Gilson, M. K.; Kim, K.; Inoue, Y. *Proc. Natl. Acad. Sci. U.S.A.* **2007**, *104*, 20737−20742.
(20) Hwang, I.; Baek, K.; Jung, M.; Kim, Y.; Park, K. M.; Lee, D. W.; Selvapalam, N.; Kim, K. *J. Am. Chem. Soc.* **2007**, *129*, 4170−4171.
(21) Eliseev, A. V.; Schneider, H.-J. *J. Am. Chem. Soc.* **1994**, *116*, 6081−6088.
(22) Florea, M.; Nau, W. M. *Org. Biomol. Chem.* **2010**, *8*, 1033−1039.
(23) Schwinte, P.; Darcy, R.; O'Keeffe, F. *J. Chem. Soc., Perkin Trans. 2* **1998**, 805−808.
(24) Mock, W. L.; Shih, N. Y. *J. Org. Chem.* **1986**, *51*, 4440−4446.
(25) Marquez, C.; Hudgins, R. R.; Nau, W. M. *J. Am. Chem. Soc.* **2004**, *126*, 5806−5816.
(26) Nau, W. M.; Florea, M.; Assaf, K. I. *Isr. J. Chem.* **2011**, *51*, 559−577.
(27) Szejtli, J. Z. *Chem. Rev.* **1998**, *98*, 1743−1754.
(28) Romero-Vargas Castrillón, S.; Giovambattista, N.; Aksay, I. A.; Debenedetti, P. G. *Chem. Phys. B* **2009**, *113*, 7973−7976.
(29) Romero-Vargas Castrillón, S.; Giovambattista, N.; Aksay, I. A.; Debenedetti, P. G. *Chem. Phys. B* **2009**, *113*, 1438−1446.
(30) Giovambattista, N.; Rossky, P. J.; Debenedetti, P. G. *Phys. Rev. Lett.* **2009**, *102*, 050603.
(31) Patel, A. J.; Varilly, P.; Chandler, D. *Chem. Phys. B* **2010**, *114*, 1632−1637.
(32) Sharma, S.; Debenedetti, P. G. *Proc. Natl. Acad. Sci. U.S.A.* **2012**, *109*, 4365−4370.
(33) Levinger, N. E. *Science* **2002**, *298*, 1722−1723.
(34) Tan, H.-S.; Piletic, I. R.; Fayer, M. D. *J. Chem. Phys.* **2005**, *122*, 174501−9.
(35) Harpham, M. R.; Ladanyi, B. M.; Levinger, N. E.; Herwig, K. W. *J. Chem. Phys.* **2004**, *121*, 7855−7868.
(36) Despa, F. *Phys. Chem. Chem. Phys.* **2008**, *10*, 4740−4747.
(37) Setny, P.; Wang, Z.; Cheng, L. T.; Li, B.; McCammon, J. A.; Dzubiella, J. *Phys. Rev. Lett.* **2009**, *103*, 187801.
(38) Baron, R.; Setny, P.; Andrew McCammon, J. *J. Am. Chem. Soc.* **2010**, *132*, 12091−12097.
(39) Mazza, M. G.; Stokely, K.; Pagnotta, S. E.; Bruni, F.; Stanley, H. E.; Franzese, G. *Proc. Natl. Acad. Sci.* **2011**, *108*, 19873−19878.
(40) Stokely, K.; Mazza, M. G.; Stanley, H. E.; Franzese, G. *Proc. Natl. Acad. Sci. U.S.A.* **2010**, *107*, 1301−1306.
(41) Stanley, H. E.; Buldyrev, S. V.; G Franzese, P. K.; Mallamace, F.; Mazza, M. G.; Stokely, K.; Xu, L. *J. Phys.: Condens. Matter* **2010**, *22*, 284101.
(42) England, J. L.; Lucent, D.; Pande, V. S. *J. Am. Chem. Soc.* **2008**, *130*, 11838−11839.
(43) Vitagliano, L.; Berisio, R.; De Simone, A. *Biophys. J.* **2011**, *100*, 2253−2261.
(44) Young, T.; Abel, R.; Kim, B.; Berne, B. J.; Friesner, R. A. *Proc. Natl. Acad. Sci. U.S.A.* **2007**, *104*, 808−813.
(45) Abel, R.; Young, T.; Farid, R.; Berne, B. J.; Friesner, R. A. *J. Am. Chem. Soc.* **2008**, *130*, 2817−2831.
(46) Beuming, T.; Farid, R.; Sherman, W. *Protein Sci.* **2009**, *18*, 1609−1619.
(47) Wang, L.; Berne, B. J.; Friesner, R. A. *Proc. Natl. Acad. Sci. U.S.A.* **2011**, *108*, 1326−1330.
(48) Hamelberg, D.; McCammon, J. A. *J. Am. Chem. Soc.* **2004**, *126*, 7683−7689.
(49) Hess, B.; Kutzner, C.; van der Spoel, D.; Lindahl, E. *J. Chem. Theory Comput.* **2008**, *4*, 435−447.
(50) Marquez, C.; Nau, W. M. *Angew. Chem., Int. Ed.* **2001**, *40*, 4387−4390.
(51) Despa, F.; Fernández, A.; Berry, R. S. *Phys. Rev. Lett.* **2004**, *93*, 228104.
(52) Koner, A. L.; Márquez, C.; Dickman, M. H.; Nau, W. M. *Angew. Chem., Int. Ed.* **2011**, *50*, 545−548.
(53) We performed an exploratory ITC measurement for complexation of DBO with CB7 in D_2O, which resulted in very small (within the error of measurements) solvent deuterium isotope effects on the thermodynamic parameters. Indeed, as was demonstrated in an extensive study with cyclodextrins, the complexation of nonionic guests and hosts is not expected to produce substantial solvent deuterium isotope effects, cf. Rekharsky, M. V.; Inoue, Y. *J. Am. Chem. Soc.* **2002**, *124*, 12361−12371.
(54) Mecozzi, S.; Rebek, J. J. *Chem.—Eur. J.* **1998**, *4*, 1016−1022.
(55) Moghaddam, S.; Inoue, Y.; Gilson, M. K. *J. Am. Chem. Soc.* **2009**, *131*, 4012−4021.
(56) Moghaddam, S.; Yang, C.; Rekharsky, M.; Ko, Y. H.; Kim, K.; Inoue, Y.; Gilson, M. K. *J. Am. Chem. Soc.* **2011**, *133*, 3570−3581.
(57) Hornak, V.; Abel, R.; Okur, A.; Strockbine, B.; Roitberg, A.; Simmerling, C. *Proteins: Struct. Funct. Bioinform.* **2006**, *65*, 712−725.
(58) Sorin, E. J.; Pande, V. S. *Biophys. J.* **2005**, *88*, 2472−2493.
(59) Horn, H. W.; Swope, W. C.; Pitera, J. W.; Madura, J. D.; Dick, T. J.; Hura, G. L.; Head-Gordon, T. *J. Chem. Phys.* **2004**, *120*, 9665−9678.
(60) Colombo, G.; Meli, M.; De Simone, A. *Proteins: Struct. Funct. Bioinform.* **2008**, *70*, 863−872.
(61) Bakirci, H. s.; Zhang, X.; Nau, W. M. *J. Org. Chem.* **2004**, *70*, 39−46.

NOTE ADDED IN PROOF

On April 16, 2012 a related study has been received by another journal, which in the meantime has appeared online: Nguyen, C. N.; Young, T. K.; Gilson, M. K., *J. Chem. Phys.* **2012**, *137*, 044101. This complementary study is limited to CB7, but reveals also a high energy as well as low entropy of the encapsulated water molecules and a toroidal cavity similar to the one depicted in the Supporting Information, Figure S2.